Defence Technology xxx (xxxx) xxx

Contents lists available at ScienceDirect

Defence Technology

journal homepage: www.keaipublishing.com/en/journals/defence-technology

Trajectory prediction algorithm of ballistic missile driven by data and knowledge

Hongyan Zang, Changsheng Gao *, Yudong Hu, Wuxing Jing

School of Astronautics, Harbin Institute of Technology, Harbin 150001, China

ARTICLE INFO

Article history:
Received 28 October 2024
Received in revised form
7 January 2025
Accepted 5 February 2025
Available online xxx

Keywords:
Ballistic missile
Trajectory prediction
The boost phase
Data and knowledge driven
The BP neural network

ABSTRACT

Recently, high-precision trajectory prediction of ballistic missiles in the boost phase has become a research hotspot. This paper proposes a trajectory prediction algorithm driven by data and knowledge (DKTP) to solve this problem. Firstly, the complex dynamics characteristics of ballistic missile in the boost phase are analyzed in detail. Secondly, combining the missile dynamics model with the target gravity turning model, a knowledge-driven target three-dimensional turning (T3) model is derived. Then, the BP neural network is used to train the boost phase trajectory database in typical scenarios to obtain a data-driven state parameter mapping (SPM) model. On this basis, an online trajectory prediction framework driven by data and knowledge is established. Based on the SPM model, the three-dimensional turning coefficients of the target are predicted by using the current state of the target, and the state of the target at the next moment is obtained by combining the T3 model. Finally, simulation verification is carried out under various conditions. The simulation results show that the DKTP algorithm combines the advantages of data-driven and knowledge-driven, improves the interpretability of the algorithm, reduces the uncertainty, which can achieve high-precision trajectory prediction of ballistic missile in the boost phase.

1. Introduction

Ballistic missile has the advantages of strong penetration capability, great lethal power, and high cost-effectiveness ratio, which has become one of the most threatening offensive weapons in modern warfare [1,2]. Therefore, the establishment of a complete missile defense system has become the focus of research of all countries [3–7]. Among the many technical links of the missile defense system, the trajectory prediction of ballistic missiles is a crucial link. Fast, high-precision trajectory prediction can provide sufficient response time for defense systems and guidance information for interceptors [8,9].

The ballistic missile flight trajectory is usually divided into boost phase, free-flight phase and reentry phase [10]. In view of the flight characteristics of these three different phases, the missile defense system has also developed three interception methods, boost interception, mid-stage interception, and terminal interception [11]. Ballistic missiles are not affected by aerodynamic forces in the free-flight phase, have a long flight time, strong trajectory regularity, and are easy to detect and predict, so the mid-course interception technology is relatively mature [12]. Ballistic missiles are affected by gravity and aerodynamic drag in the reentry phase, and through the improvement and optimization of the low-level air defense system, the terminal interception technology has also been rapidly developed, forming a terminal defense system with operational flexibility [13]. However, the latter two interception methods also have some disadvantages, such as the decoy and warhead released in the free-flight phase will bring difficulties to target identification, and the reentry phase of the ballistic missile is too fast, making interception more difficult. In contrast, the boost phase interception has many advantages [11]: 1) The engine tail flame of the ballistic missile is conducive to detection and stable tracking. 2) The flight speed is relatively low. 3) There is no deception interference in the boost phase flight, and all warheads can be destroyed if the interception is successful. 4) Secondary interception can be carried out if the interception is unsuccessful. Based on the above considerations, scholars have gradually devoted their energy to the research work of the boost phase interception [14–17]. To establish the complete missile defense system and provide accurate and reliable trajectory prediction information for

* Corresponding author.
E-mail address: gaocs@hit.edu.cn (C. Gao).
Peer review under the responsibility of China Ordnance Society.

https://doi.org/10.1016/j.dt.2025.02.001

boost phase interception, this paper studies the problem of high-precision trajectory prediction of the boost phase.

At present, trajectory prediction algorithms are mainly divided into two categories, knowledge-driven and data-driven. The knowledge-driven trajectory prediction algorithms can make full use of existing knowledge, including existing model and algorithm knowledge, rule experience knowledge, and domain-specific knowledge [18–20]. Knowledge-driven methods can deeply integrate multidisciplinary knowledge. A perfect theoretical system helps to establish an accurate model, and the algorithm has good stability [21,22]. Knowledge-driven trajectory prediction algorithms are widely used in trajectory prediction of hypersonic vehicles. Li et al. [23] fully analyzed the motion characteristics of the near space hypersonic vehicle (NSHV), and selected the flight state as the prediction parameter. Then they used Hough transform to detect the time series of different parameters, and predicted the trajectory according to the fitting function. Hu et al. [24] established a maneuvering mode parameter model based on the autoregressive method to mine the historical data of the aircraft. On this basis, Bayesian estimation theory is used to predict the intention to deal with the sudden change of maneuver mode. For ballistic missiles, knowledge-based trajectory prediction algorithms are mostly used to predict the trajectory of the free-flight phase and the reentry phase. The commonly used methods include the analytical method [18], the numerical integration method [19], and the function approximation method [25]. Compared with the free-flight phase and the reentry phase, the trajectory prediction of ballistic missiles in the boost phase is affected by unknown forces such as thrust, aerodynamic drag and gravity. Therefore, trajectory prediction at this phase is more challenging. Due to the complexity of the force, the applicability of knowledge-driven trajectory prediction models, such as polynomial prediction models and target gravity turning models, is reduced, and it is difficult to accurately describe the motion characteristics in the boost phase [10]. In recent years, data-driven trajectory prediction algorithms have developed rapidly. The data-driven method directly constructs the corresponding mapping relationship through the database, which does not require accurate modeling [26,27]. It can continuously learn and evolve from the data, and the algorithm has strong versatility [28–30]. Commonly used data-driven trajectory prediction methods include BP neural networks [31], convolutional neural networks [32], recurrent neural networks [16], and Gaussian process regression [33]. Researchers can design and improve corresponding intelligent algorithms according to specific problems. However, with the increasing complexity of the problem, problems such as dimensional disasters and over-reliance on huge computing power have brought severe challenges to data-driven trajectory prediction. At the same time, the current data-driven method has some problems, such as the lack of clarity of physical meaning and the large demand for high-quality data. For objects such as ballistic missiles, which have complex flight environments and are not rich in historical data, their engineering application is difficult.

Through the above analysis, there are certain deficiencies and defects in both data-driven method and knowledge-driven method. Combining them can make full use of their respective advantages and further enhance the performance of the algorithm [34,35]. The data-driven method has the characteristics of strong nonlinear expression ability and offline/online learning, which can make up for the limitations of the knowledge-driven method under the complexity of the model, the absence of accurate modeling, and the uncertainty of the environment. The knowledge-driven method can decompose and reduce the dimension of complex problems, or optimize the initial parameter value and learning architecture of the data-driven method, which is conducive to the convergence of data-driven methods. At present, the method driven by the mixture of data and knowledge is widely used in the field of aircraft control [36], but it is rarely used in the field of aircraft trajectory prediction. Therefore, this paper combines data-driven and knowledge-driven, and proposes a trajectory prediction algorithm for ballistic missiles driven by data and knowledge (DKTP).

1) Aiming at the problem of acceleration abrupt change caused by interstage switching of multi-stage ballistic missile and the change of flight procedures, this paper combines the dynamics model in the boost phase with the gravity turning (GT) model of the target to derive the three-dimensional turning (T3) model. The T3 model can accurately describe the three-dimensional motion trajectory in the boost phase.
2) Combined with the dynamics model in the boost phase and the T3 model, the three-dimensional turning parameters during the flight in the boost phase is extracted and analyzed. The three-dimensional turning parameters can accurately reflect the thrust change of the boost phase engine and the change of flight program.
3) The relationship between the three-dimensional turning parameter and the flight state is derived, and the state-parameter mapping (SPM) model in the boost phase is established based on the trajectory database and the BP neural network. The SPM model takes the current state of the target as the input and the target three-dimensional turning coefficient as the output. Combined with the SPM model and the T3 model, the trajectory in the boost phase can be predicted online.

The rest of this article is organized as follows. A typical trajectory prediction scenario in the boost phase based on the air-based dual infrared detector is established in Section 2. In Section 3, the DKTP algorithm is designed. The results of the numerical simulations are presented in Section 4. Finally, Section 5 presents the conclusion.

2. Problem description

As shown in Fig. 1, in this paper, the air-based dual infrared detector is used to continuously track the ballistic missile to time T_t, and then predicts the flight trajectory of any future time $T_t < t < T_p$. To accomplish this, this section provides the motion model and measurement model for ballistic missile in the boost phase.

2.1. Motion model

The motion model of ballistic missile in boost phase is established based on a 6-degree-of-freedom simulation model, which considers the Earth's rotation and treats it as a standard ellipsoid. During the flight in the boost phase, the missile is mainly affected by gravity, engine thrust and aerodynamic force. Ignoring the control force and its torque effect. According to the Newton's second law and the vector derivation rule, the dynamics equation for the centroid of a missile in the launch coordinate system is [10].

$$m\frac{\delta^2 \boldsymbol{r}}{\delta t^2} = \boldsymbol{P} + \boldsymbol{R} + m\boldsymbol{g} - 2m\omega_e \times \frac{\delta \boldsymbol{r}}{\delta t} - m\omega_e \times (\omega_e \times \boldsymbol{r}) \tag{1}$$

where $\boldsymbol{r}$ is the vector from the center of the earth to the current position of the missile. $\boldsymbol{R}$ is the aerodynamic vector acting on the missile. $\boldsymbol{P}$ is the engine thrust vector. m is the current missile mass. $\boldsymbol{g}$ is the gravitational acceleration. ω_e is the rotational angular velocity of the launch coordinate system relative to the geocentric inertial coordinate system (ECI-CS).

Then, the dynamics equation for the centroid of a missile is:

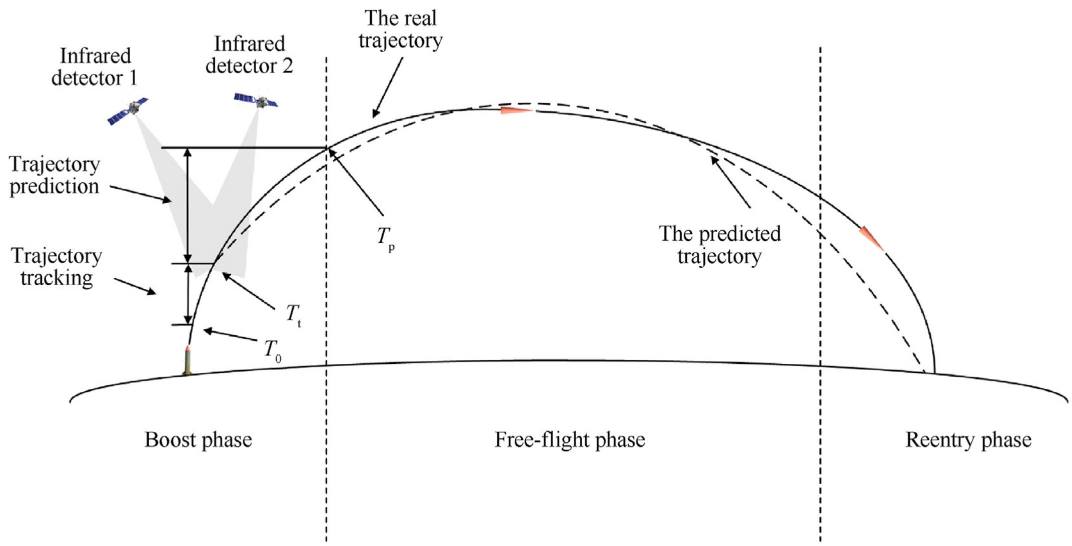

Fig. 1. Schematic diagram of boost phase trajectory prediction.

$$m\begin{bmatrix}\dfrac{\mathrm{d}v_x}{\mathrm{d}t}\\ \dfrac{\mathrm{d}v_y}{\mathrm{d}t}\\ \dfrac{\mathrm{d}v_z}{\mathrm{d}t}\end{bmatrix}=\boldsymbol{\Gamma}_{10}\begin{bmatrix}P\\0\\0\end{bmatrix}+\boldsymbol{\Gamma}_{13}\begin{bmatrix}-C_x qS_M\\ C_y^{\alpha} qS_M\alpha\\ C_x^{\beta} qS_M\beta\end{bmatrix}+m\frac{g_r'}{r}\begin{bmatrix}x+R_{ox}\\ y+R_{oy}\\ z+R_{oz}\end{bmatrix}$$
$$+m\frac{g_{\omega e}}{\omega_e}\begin{bmatrix}\omega_{ex}\\ \omega_{ey}\\ \omega_{ez}\end{bmatrix}-m\begin{bmatrix}a_{ex}\\ a_{ey}\\ a_{ez}\end{bmatrix}-m\begin{bmatrix}a_{kx}\\ a_{ky}\\ a_{kz}\end{bmatrix} \tag{2}$$

where $\begin{bmatrix}\mathrm{d}v_x/\mathrm{d}t & \mathrm{d}v_y/\mathrm{d}t & \mathrm{d}v_z/\mathrm{d}t\end{bmatrix}^{\mathrm{T}}$ is the component of the relative acceleration term in the launch coordinate system. $\boldsymbol{\Gamma}_{10}=\boldsymbol{\Gamma}_{01}^{-1}$ is the conversion matrix from the body coordinate system to the launch coordinate system. P is the thrust. $\boldsymbol{\Gamma}_{13}=\boldsymbol{\Gamma}_{31}^{-1}$ is the conversion matrix from the velocity coordinate system to the launch coordinate system. $\begin{bmatrix}C_x & C_y^{\alpha} & C_x^{\beta}\end{bmatrix}^{\mathrm{T}}$ is the aerodynamic coefficient. q is the dynamic head. S_M is the characteristic area. α and β are the angle of attack and sideslip angle respectively. g_r' and $g_{\omega e}$ are the gravitational acceleration terms. $\begin{bmatrix}R_{ox} & R_{oy} & R_{oz}\end{bmatrix}^{\mathrm{T}}$ is the component of the launch point geocentric vector $\boldsymbol{R}_0$ in the launch coordinate system. $\begin{bmatrix}\omega_{ex} & \omega_{ey} & \omega_{ez}\end{bmatrix}^{\mathrm{T}}$ is the component of $\boldsymbol{\omega}_e$ in the launch coordinate system. $\begin{bmatrix}a_{ex} & a_{ey} & a_{ez}\end{bmatrix}^{\mathrm{T}}$ is the centrifugal inertial acceleration, and $\begin{bmatrix}a_{kx} & a_{ky} & a_{kz}\end{bmatrix}^{\mathrm{T}}$ is the Coriolis inertial acceleration.

The kinematic equation for the centroid is:

$$\begin{cases}\dfrac{\mathrm{d}x}{\mathrm{d}t}=v_x\\ \dfrac{\mathrm{d}y}{\mathrm{d}t}=v_y\\ \dfrac{\mathrm{d}z}{\mathrm{d}t}=v_z\end{cases} \tag{3}$$

The boost phase motion model of ballistic missiles can provide a basis for the generation of ballistic databases, and can also be used to provide guidance for the design of target state/parameter joint estimation trackers.

2.2. Measurement model

Because the ballistic missile engine produces a large amount of high-temperature tail flames when working, it has obvious infrared characteristics and is easy to be detected and tracked by infrared detectors. As shown in Fig. 2, this paper will use the air-based infrared detector to detect the boost phase of the missile, which can effectively make up for the shortcomings of the early warning capability of land/sea-based early warning platforms. Compared with space-based early warning systems, air-based early warning and detection systems are highly mobile which can be lifted into the air within hours or even minutes, and are not affected by atmospheric refraction [37].

In this paper, the dual infrared measurement model is adopted. The detection model describes the relationship between the position of the aircraft and the detection data of the detector. The general expression for the dual infrared measurement model is [37].

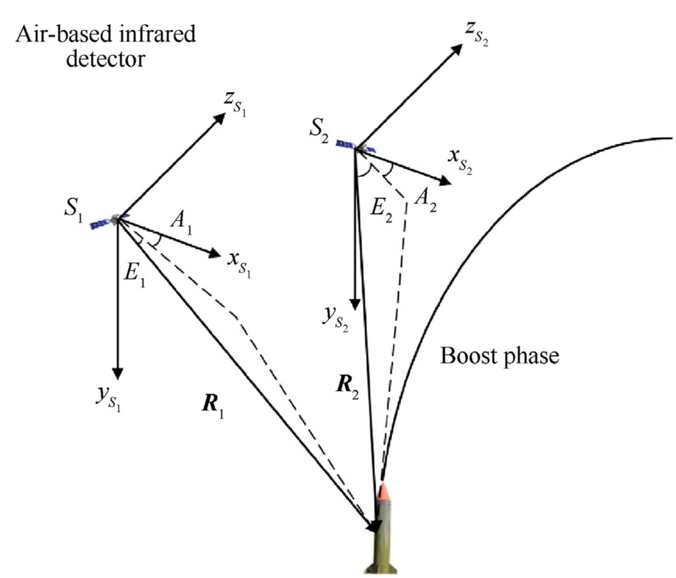

Fig. 2. Schematic diagram of air-based early warning platform detection.

$$\boldsymbol{Y}_i = (A_{1,i}, E_{1,i}, A_{2,i}, E_{2,i}) = \boldsymbol{h}(\boldsymbol{X}_i) \tag{4}$$

where $A_{1,i}, E_{1,i}$ is the azimuth angle and the altitude angle obtained by the first detector S_1 at i moments respectively. $A_{2,i}, E_{2,i}$ is the azimuth angle and the altitude angle obtained by the second detector S_2 at i moments respectively, and $\boldsymbol{X}_i$ is the state vector of the target at i moment.

Suppose that the coordinates of the aircraft and the detector S_n are $[x \quad y \quad z]^{\mathrm{T}}$ and $[x \quad y \quad z]_{S_n}^{\mathrm{T}}$, respectively, in the Earth-centered fixed coordinate system (ECF-CS). Then the component of the line-of-sight vector of the aircraft relative to the detector in the detection coordinate system is:

$$\Delta \boldsymbol{R}_{S_n} = \begin{bmatrix} x_n \\ y_n \\ z_n \end{bmatrix} = \boldsymbol{\Gamma}_{\mathrm{E}}^{S_n} \left(\begin{bmatrix} x \\ y \\ z \end{bmatrix} - \begin{bmatrix} x \\ y \\ z \end{bmatrix}_{S_n} \right), n = 1, 2 \tag{5}$$

where $\boldsymbol{\Gamma}_{\mathrm{E}}^{S_n}$ is the conversion matrix from ECF-CS to the detection coordinate system. The formula for calculating the azimuth angle and the altitude angle is:

$$\begin{cases} A_n = \arctan\left(-\dfrac{z_n}{x_n}\right) \\ E_n = \arctan\left(\dfrac{y_n}{\sqrt{x_n^2 + y_n^2}}\right) \end{cases} \tag{6}$$

Eqs. (4) and (6) constitute the analytical formula of the measurement model.

3. Trajectory prediction algorithms driven by data and knowledge

The framework of the trajectory prediction algorithm driven by data and knowledge (DKTP) is established, as shown in Fig. 3. The DKTP algorithm consists of three parts. The first is the knowledge-driven part. Considering the abrupt acceleration in the boost phase, the traditional trajectory prediction model cannot accurately describe the motion characteristics in the boost phase. Therefore, based on the dynamics model of the boost phase and the GT model, the T3 model is derived, and the three-dimensional turning parameter is extracted. The second is the data-driven part. Trajectory database is established based on the dynamics model in the boost phase. The T3 model and BP neural network are used to train the trajectory database to obtain the boost phase SPM model. Finally, the knowledge-driven and data-driven are combined, and the turning parameter at the current moment is predicted by the current moment state of the aircraft obtained by tracking. On this basis, the next moment state of the target is obtained by combining the turning parameter at the current moment and the T3 model, and it is continuously iterated until the end of the forecast.

3.1. The three-dimensional turning model

3.1.1. Analysis of the dynamics characteristics

The dynamics of the multi-stage ballistic missile in the boost phase is essentially a process of variable mass motion, and the acceleration of each stage changes slowly with the change of mass. However, there are mass abrupt changes and thrust abrupt changes at the shutdown points at all levels, which will cause drastic changes of the acceleration in the interstage switching stage. In addition, the guidance and control of the boost phase also makes it difficult to give a clear law of acceleration motion. Multi-stage booster ballistic missiles have fast speed, complex maneuvering characteristics, and difficult prediction, so it is necessary to analyze the motion characteristics in the boost phase.

During the flight of the ballistic missile in the boost phase, it is mainly affected by the engine thrust, aerodynamic force and the Earth's gravity, among which the engine thrust accounts for the largest proportion. According to the flight characteristics in the boost phase, it can be divided into the vertical flight segment, the turning segment and the aiming segment. The vertical flight section is the first stage after the missile is launched, which generally only takes a few seconds, and its purpose is to ensure the stability of the missile's take-off and make the engine enter the rated working state. After the end of the vertical ascent stage, the missile flies into the turning section. The turning section is divided into the negative angle of attack turning section and the gravity turning section. In this stage, under the action of the guidance system, the missile deflects from the vertical flight state to the target direction. The missile must turn according to the prescribed procedure to hit the target accurately. The last section is the aiming section, which is the section from the end of the turning section to the shutdown point. The main purpose of this section is to control the speed of shutdown points to control the range of missiles. Generally, the pitch angle can be used as a control quantity for ballistic design. The variation law of the pitch angle in the boost phase is shown in Fig. 4.

The kinetic characteristics in the boost phase of a typical long-range ballistic missile are analyzed below. The ballistic missile is a three-stage booster missile. The end time of the first-stage booster is 75 s, the end time of the second-stage booster is 155 s, and the end time of the third-stage booster which is the moment the engine turned off is 201 s. Figs. 5 and 6 show the velocity curves in the boost phase. Figs. 7 and 8 show the acceleration curves in the boost phase.

From the above simulation results, in addition to the abrupt change of acceleration during inter-stage switching, the acceleration curve will also fluctuate with the change of flight procedure such as the turning section of negative angle of attack, the turning section of gravity and the initial stage of aiming section. These bring great challenges to the trajectory prediction in the booster section. Therefore, it is necessary to establish a target motion model that can accurately describe the acceleration change in the boost phase.

3.1.2. Model building and parameter extraction

During the flight of the boost phase, the engine thrust makes the target accelerate the flight. The gravity and aerodynamic force make the target turn. The typical ballistic missile maintains zero angle of attack, following a gravity-turning trajectory. According to the characteristics of the motion in the boost phase, it is suitable to use the GT model to describe the target motion [10]. The core idea of the GT model is assumed that in ECF-CS, the total force experienced by the missile other than gravity is parallel to the relative velocity vector. That is, the nongravitational net acceleration $\boldsymbol{a}_N$ of the target in ECF-CS is parallel to the velocity $\boldsymbol{v}$. Define a scaling factor k that satisfies [10]:

$$\boldsymbol{a}_N = k\boldsymbol{v} \tag{7}$$

where k is called the gravitational turning parameter. Expand Eq. (7) to obtain

$$\begin{cases} a_{Nx} = kv_x \\ a_{Ny} = kv_y \\ a_{Nz} = kv_z \end{cases} \tag{8}$$

When k is unknown, extend k to the state quantity. the state quantity is:

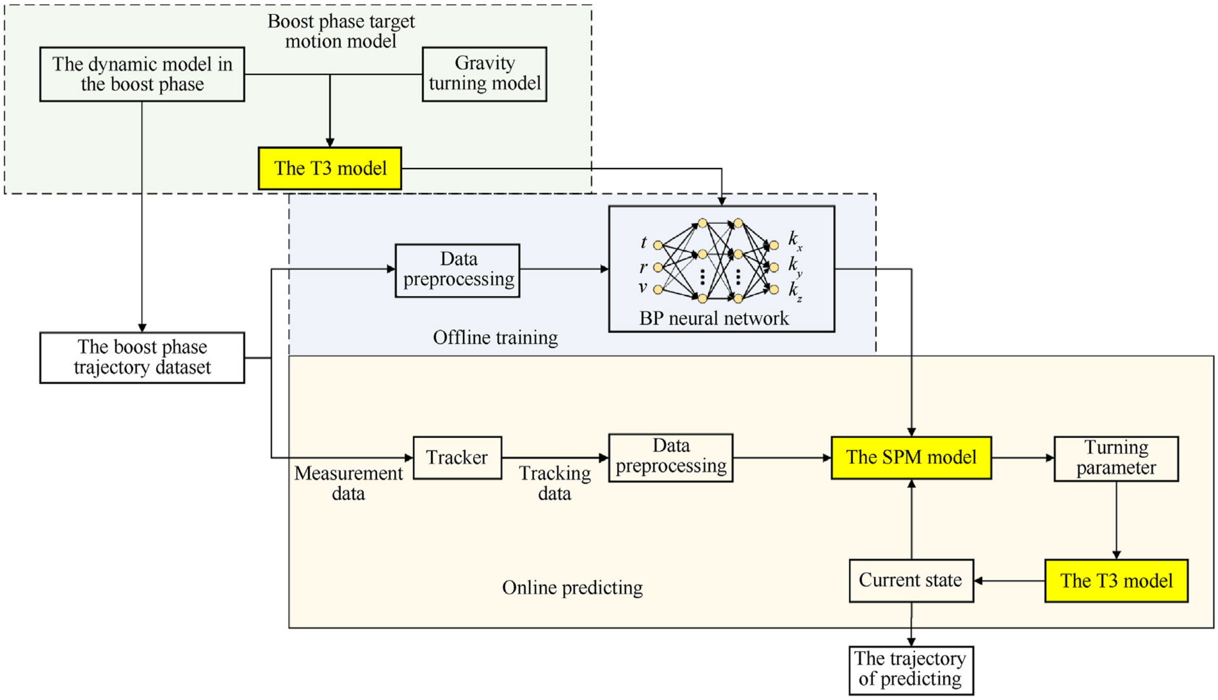

Fig. 3. Block diagram of the trajectory prediction algorithm driven by data and knowledge.

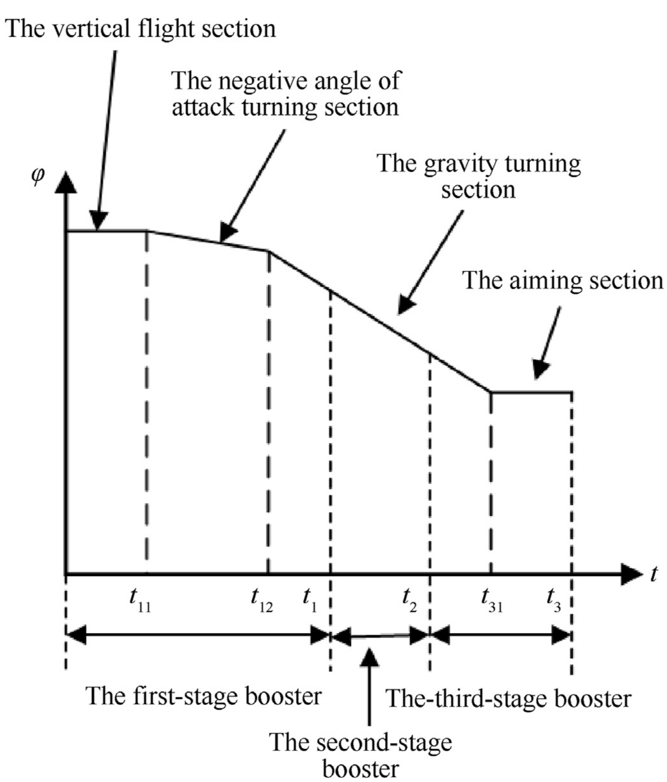

Fig. 4. Flight procedure of pitch angle in boost phase of ballistic missile.

$$\boldsymbol{X} = [x, y, z, v_x, v_y, v_z, k]^{\mathrm{T}} \tag{9}$$

Considering the system noise, the GT model is:

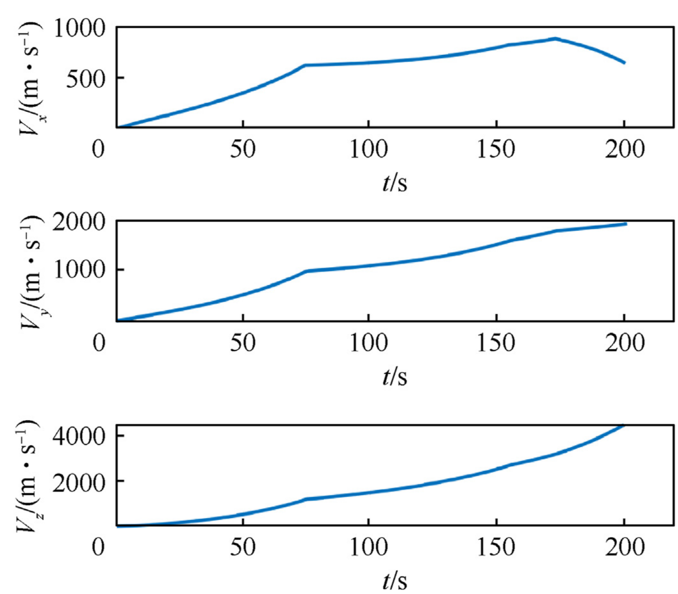

Fig. 5. The three-dimensional velocity curve in the boost phase.

$$\begin{cases} \dot{x} = v_x \\ \dot{y} = v_y \\ \dot{z} = v_z \\ \dot{v}_x = kv_x + a_{G_x} + w_x \\ \dot{v}_y = kv_y + a_{G_y} + w_y \\ \dot{v}_z = kv_z + a_{G_z} + w_z \\ \dot{k} = 0 + w_k \end{cases} \tag{10}$$

where $\boldsymbol{a}_G = -\mu\boldsymbol{p}/p^3 = [a_{Gx}, a_{Gy}, a_{Gz}]^{\mathrm{T}}$, $\boldsymbol{p} = [x, y, z]^{\mathrm{T}}$. The system noise is $w_i (i = x, y, z, k)$.

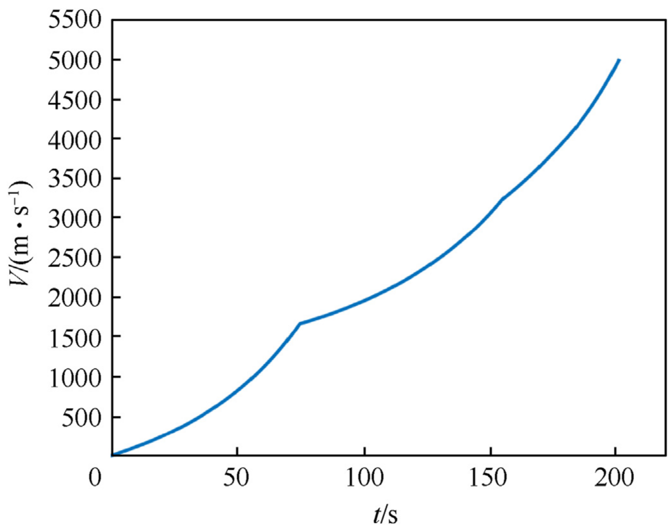

Fig. 6. The velocity curve in the boost phase.

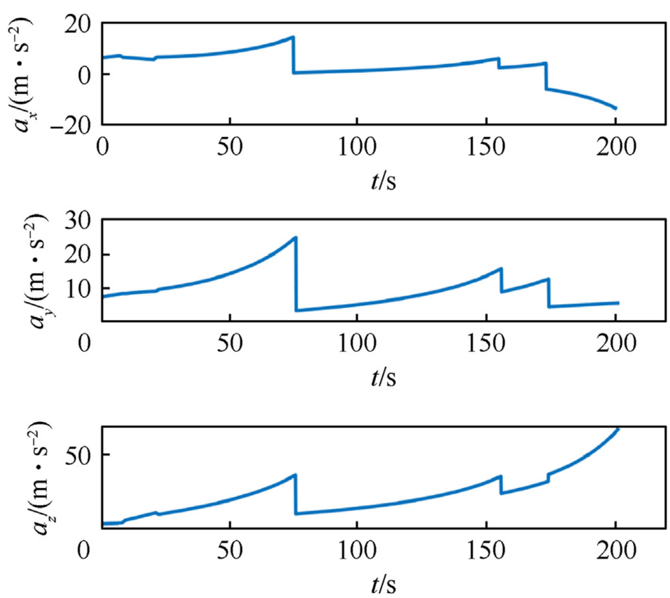

Fig. 7. The three-dimensional acceleration curve in the boost phase.

Mass abrupt changes and thrust abrupt changes occur during the switching between the boost phase of a multi-stage ballistic missile, which will lead to drastic changes in the acceleration in the boost phase. At the same time, the change of flight procedure in the boost phase will also bring difficulties to accurately describe the acceleration change of the target. At this point, the GT model can no longer accurately describe the movement of the target. Therefore, this paper improves the GT model.

Defining $\boldsymbol{K}$ as the three-dimensional turning parameter:

$$\begin{cases} k_x = \dfrac{a_{Nx}}{v_x} \\ k_y = \dfrac{a_{Ny}}{v_y} \\ k_z = \dfrac{a_{Nz}}{v_z} \end{cases} \tag{11}$$

Then the three-dimensional turning (T3) model in the target

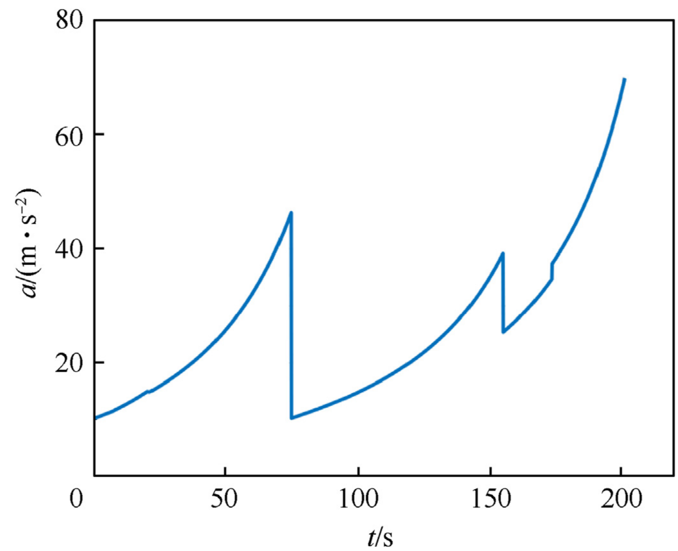

Fig. 8. The acceleration curve in the boost phase.

boost phase is obtained as follows:

$$\begin{cases} \dot{x} = v_x \\ \dot{y} = v_y \\ \dot{z} = v_z \\ \dot{v}_x = k_x v_x + a_{G_x} + w_x \\ \dot{v}_y = k_y v_y + a_{G_y} + w_y \\ \dot{v}_z = k_z v_z + a_{G_z} + w_z \\ \dot{k}_x = 0 + w_{k_x} \\ \dot{k}_y = 0 + w_{k_y} \\ \dot{k}_z = 0 + w_{k_z} \end{cases} \tag{12}$$

where $w_i(i = x, y, z, k_x, k_y, k_z)$ is the system noise. $\boldsymbol{K} = (k_x, k_y, k_z)$ is the ratio of the nongravitational net acceleration component (a_{Nx}, a_{Ny}, a_{Nz}) to the velocity component (v_x, v_y, v_z) of the target in ECF-CS.

$\boldsymbol{K}$ is analyzed below. A typical three-stage booster ballistic missile is selected, and the launch conditions are the same as those set in the analysis of the kinetic characteristics in the boost phase. The acceleration and the nongravitational net acceleration in the boost phase are obtained as shown in Figs. 9 and 10. It can be seen they have the same change trend. This fully illustrates the equivalence of the description of missile maneuverability by using acceleration and the nongravitational net acceleration as maneuvering parameters. However, the gravity model needs to be constructed for acceleration estimation, and the gravity model in the boost phase is more complex, so it is more advantageous to choose the nongravitational net acceleration as the maneuvering parameter estimation. At the same time, the nongravitational net acceleration curve is smoother at all levels, which is more helpful for trajectory prediction.

The Comparison of $\boldsymbol{K}$ in the boost phase is obtained as shown in Fig. 11. From comparison chart of the three-dimensional turning parameter $\boldsymbol{K}$ and the gravity turning parameter k, it can be seen that there are significant differences between $\boldsymbol{K}$ and k in the aiming section of the multi-stage booster ballistic missile. It shows that the GT cannot accurately express the acceleration characteristics of ballistic missiles in the aiming section, and there are algorithm limitations. However, the T3 model feeds back the three-axis acceleration respectively, which has higher model accuracy.

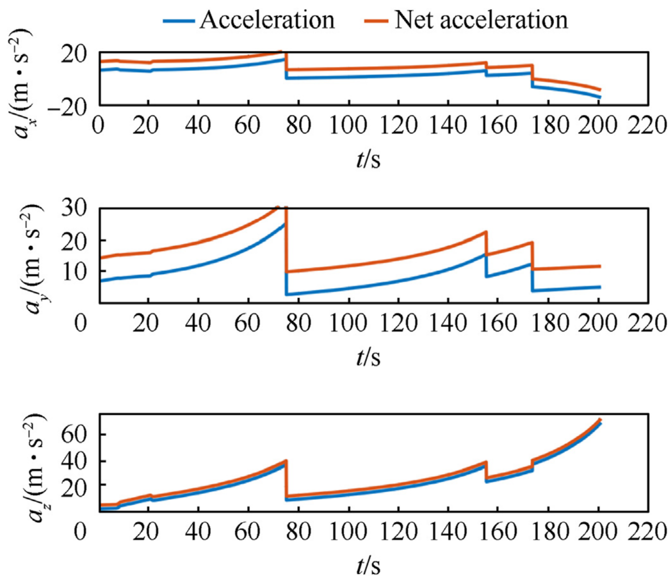

Fig. 9. Comparison of the three-dimensional acceleration curves.

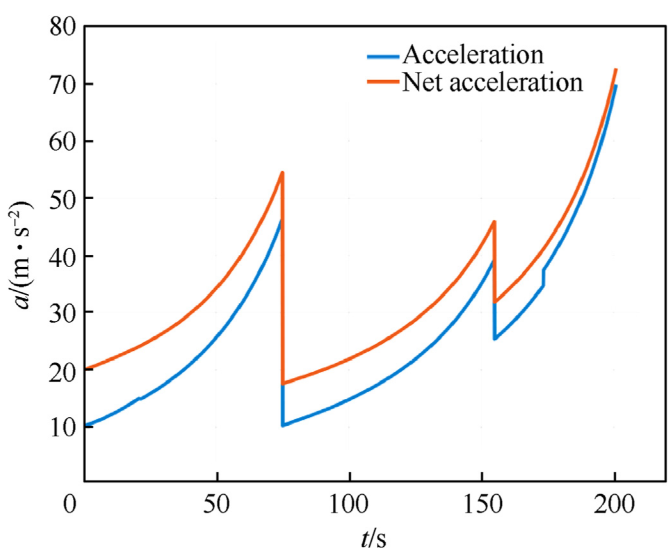

Fig. 10. Comparison of the acceleration curves.

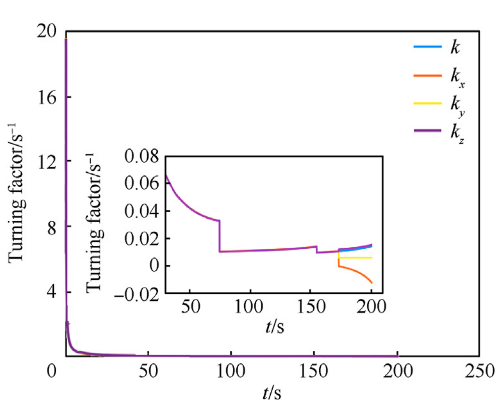

Fig. 11. Comparison of the turning parameter curves.

3.2. The state-parameter mapping model

3.2.1. Model building

After obtaining the T3 model, the state-parameter mapping (SPM) model will be established. The trajectory dataset is used to study the flight law of the boost phase. The relationship between $\boldsymbol{K}$ and the target engine working time, target position and speed is obtained by fitting. From Eq. (1), the nongravitational net acceleration in the boost phase is:

$$\boldsymbol{a}_N = \frac{\boldsymbol{P} + \boldsymbol{R} - 2m\omega_e \times \frac{\delta \boldsymbol{r}}{\delta t} - m\omega_e \times (\omega_e \times \boldsymbol{r})}{m} \tag{13}$$

Expand Eq. (13) in the launch coordinate system:

$$\boldsymbol{a}_N = \frac{\boldsymbol{\Gamma}_{10}}{m}\begin{bmatrix} P \\ 0 \\ 0 \end{bmatrix} + \frac{\boldsymbol{\Gamma}_{13}}{m}\begin{bmatrix} -C_x q S_M \\ C_y^{\alpha} q S_M \alpha \\ C_x^{\beta} q S_M \beta \end{bmatrix} - \begin{bmatrix} a_{ex} \\ a_{ey} \\ a_{ez} \end{bmatrix} - \begin{bmatrix} a_{kx} \\ a_{ky} \\ a_{kz} \end{bmatrix} \tag{14}$$

The nongravitational net acceleration in the launch coordinate system is converted to ECF-CS to obtain:

$$\boldsymbol{a}_N = \frac{\boldsymbol{\Gamma}_{\mathrm{E}1}\boldsymbol{\Gamma}_{10}}{m}\begin{bmatrix} P \\ 0 \\ 0 \end{bmatrix} + \frac{\boldsymbol{\Gamma}_{\mathrm{E}1}\boldsymbol{\Gamma}_{13}}{m}\begin{bmatrix} -C_x q S_M \\ C_y^{\alpha} q S_M \alpha \\ C_x^{\beta} q S_M \beta \end{bmatrix} - \boldsymbol{\Gamma}_{\mathrm{E}1}\begin{bmatrix} a_{ex} \\ a_{ey} \\ a_{ez} \end{bmatrix} - \boldsymbol{\Gamma}_{\mathrm{E}1}\begin{bmatrix} a_{kx} \\ a_{ky} \\ a_{kz} \end{bmatrix} \tag{15}$$

where $\boldsymbol{\Gamma}_{\mathrm{E}1}$ is the conversion matrix from the launch system to ECF-CS. Then the formula for calculating $\boldsymbol{K}$ can be obtained as follows:

$$\boldsymbol{K} = \frac{\boldsymbol{a}_N}{\boldsymbol{v}} = \frac{\boldsymbol{\Gamma}_{\mathrm{E}1}\boldsymbol{\Gamma}_{10}}{m\boldsymbol{v}}\begin{bmatrix} P \\ 0 \\ 0 \end{bmatrix} + \frac{\boldsymbol{\Gamma}_{\mathrm{E}1}\boldsymbol{\Gamma}_{13}}{m\boldsymbol{v}}\begin{bmatrix} -C_x q S_M \\ C_y^{\alpha} q S_M \alpha \\ C_x^{\beta} q S_M \beta \end{bmatrix} - \frac{\boldsymbol{\Gamma}_{\mathrm{E}1}}{\boldsymbol{v}}\begin{bmatrix} a_{ex} \\ a_{ey} \\ a_{ez} \end{bmatrix} - \frac{\boldsymbol{\Gamma}_{\mathrm{E}1}}{\boldsymbol{v}}\begin{bmatrix} a_{kx} \\ a_{ky} \\ a_{kz} \end{bmatrix} \tag{16}$$

As can be seen from the calculation formula of $\boldsymbol{K}$, $\boldsymbol{K}$ is related to the prior information thrust of the target p, the state information position $\boldsymbol{r}$, and the velocity $\boldsymbol{v}$. Among them, the thrust P is related to the engine operating time t. Therefore, the SPM model is established as follows:

$$\boldsymbol{K} = [k_x, k_y, k_z] = f(t, \boldsymbol{r}, \boldsymbol{v}) \tag{17}$$

Through the above analysis, it can be seen the SPM model should be a seven-input and three-output model. The structure of the SPM model is shown in Fig. 12.

3.2.2. Network structure

Due to the complexity of the mapping model, it is not possible to give an analytical solution directly. In this paper, we will use the powerful learning ability of neural networks to establish a mapping model between motion state and $\boldsymbol{K}$. Because of the unique error back propagation training method of BP neural network, the problem that the connection weight of hidden layer of neural network can not be adjusted is successfully solved [38]. This paper uses the BP neural network to train the SPM model.

The main idea of BP neural network is to compare the results obtained by the output layer with the expected output, and use the

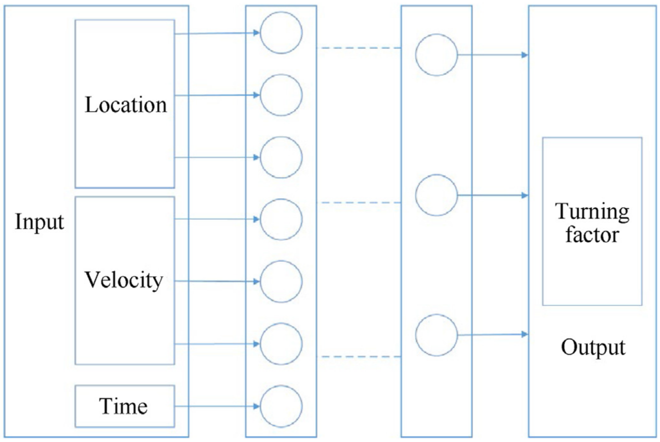

Fig. 12. Structure diagram of the SPM model.

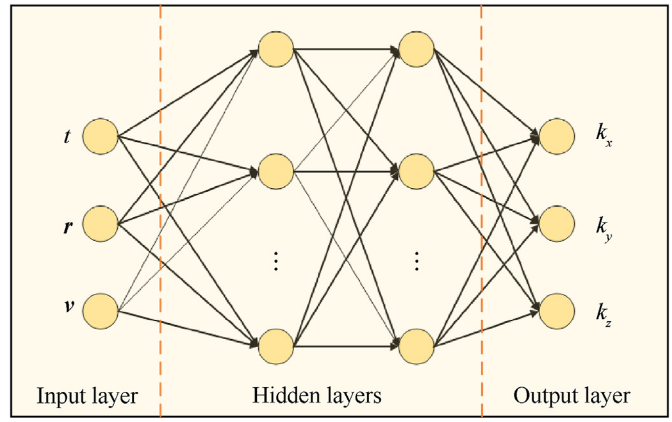

Fig. 13. Structure diagram of BP neural network.

error to adjust the weights between the hidden layer and each neuron. It consists of two processes: the forward propagation of the input signal and the back propagation of the output result error [38]. Defines the output error as:

$$E = \frac{1}{2}(\boldsymbol{D} - \boldsymbol{d})^2 = \frac{1}{2}\sum_{k=1}^{l}(D_k - d_k)^2 \tag{18}$$

where d is the output value. D is the expected output, and l is the output dimension.

The error is propagated back to the hidden layer as:

$$E = \frac{1}{2}\sum_{k=1}^{l}\left(D_k - F\left(\sum_{j=1}^{m} u_{jk}y_j - c\right)\right)^2 \tag{19}$$

where m is the number of neurons in the hidden layer. u is the weight corresponding to the connection of neurons from the hidden layer to the output layer. c is the threshold.

The error is propagated back from the hidden layer to the input layer:

$$E = \frac{1}{2}\sum_{k=1}^{l}\left(D_k - F\left(\sum_{j=1}^{m} u_{jk}F\left(\sum_{i=1}^{n} w_{ij}x_i - b\right) - c\right)\right)^2 \tag{20}$$

It can be seen from the above formula that the output error is a function of the weight w between the input layer and the hidden layer, and the weight u between the hidden layer and the output layer. The range of output error can be adjusted by adjusting the weight. In order to achieve the approximation of the input-output relationship, the output error should be minimized by adjusting the weight. Therefore, the weight adjustment method between layers can be selected as:

$$\begin{cases} \Delta w_{jk} = -\eta \dfrac{\partial E}{\partial w_{jk}} & j = 1,2,\cdots,m; k = 1,2,\cdots,l \\ \Delta u_{ij} = -\eta \dfrac{\partial E}{\partial u_{ij}} & i = 1,2,\cdots,n; j = 1,2,\cdots,m \end{cases} \tag{21}$$

where η is Learning rate.

The structure of the BP neural network used in this paper is shown in Fig. 13. The input is the prior information and the state information of the target $(t, \boldsymbol{r}, \boldsymbol{v})$, the output is $\boldsymbol{K} = [k_x, k_y, k_z]$, and the hidden layer is selected as two layers. When training a neural network, the parameters in the neural network are divided into two categories. One is parameters that can be updated by way of learning, such as weights between neurons ω and biases of neurons b. The other type of parameters cannot be updated by learning, which are called hyperparameters, such as the number of neuronal nodes between layers, the number of hidden layers, and the learning rate. In this paper, the hyperparameters are determined by multiple simulations. Finally, the number of nodes in hidden layer 1 is 60, and the number of nodes in hidden layer 2 is 18. By preparing a large amount of data to train the above-mentioned neural network, the neural network obtained after determining the weights of each layer can realize the approximation of the model parameter $\boldsymbol{K}$. In this paper, the scheme of offline training network and online trajectory prediction is adopted.

3.2.3. Generation and processing of trajectory dataset in the boost phase

In the training of neural networks, the more complex the relationship between input and output, the more sample data is required, and the randomness and balance of sample data must be ensured. In this paper, the optimal trajectory under different launch points and target points is selected as the sample trajectory. Taking a certain type of mobile-launched intercontinental ballistic missile (ICBM) as the research object, the launch point and target point of the missile are randomly generated by uniform distribution. At the same time, from the perspective of the defense side, the incoming ballistic missile target is a non-cooperative target. This means that its model parameters cannot be fully grasped. Therefore, the parameters that have a greater impact on the trajectory shape of the target 's boost phase, such as engine working time, thrust, and aerodynamic coefficient, will be randomly deflected to varying degrees. Table 1 shows the parameter of trajectory dataset, including the range of launch point, the range of target point, and the degree of parameter deviation.

In the range of the launch point and the target point shown in Table 1, the trajectory dataset of the boost phase is obtained by planning the missile launch data. As shown in Fig. 14, 1000 trajectories are obtained to construct a trajectory dataset of the boost phase, including 500 trajectories generated by standard parameters and 500 trajectories generated by deviation parameters. It can be seen from Fig. 14 that the trajectory dataset of the boost phase contains all the typical trajectories of the boost phase as much as possible. In the boost phase trajectory dataset, 70% is randomly selected as the training set, 15% as the test set, and 15% as the verification set.

According to the characteristics of the sample data, it is usually

Table 1
Parameter of trajectory dataset.

Parameter	Value
Longitude of the launch point/(°)	[45 50]
Latitude of the launch point/(°)	[15 20]
Altitude of the launch point/m	[0 1000]
Longitude of the target point/(°)	[60 65]
Latitude of the target point/(°)	[45 53]
Altitude of the target point/m	[0 1000]
Range/km	[2965.7 4523.1]
The maximum deviation percentage of engine working time/%	10
The maximum deviation percentage of thrust/%	10
The maximum deviation percentage of aerodynamic coefficient/%	10

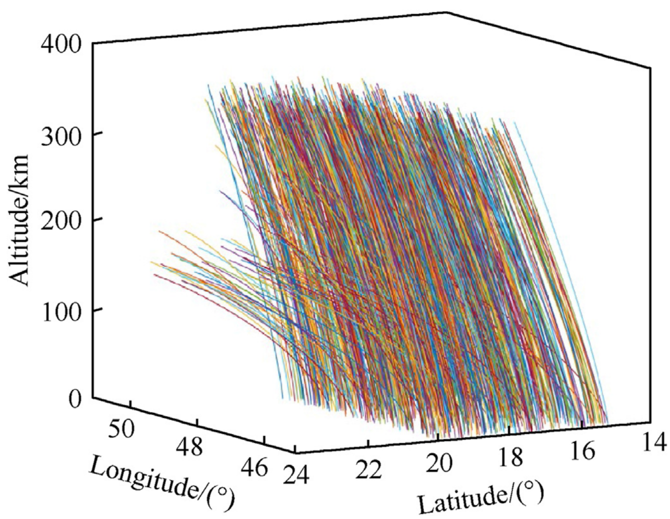

Fig. 14. Trajectory dataset in the boost phase.

necessary to normalize the data. Map the data to the interval $[-1, 1]$ and calculate it as follows:

$$\begin{cases} x_{\text{mid}} = \dfrac{x_{\max} + x_{\min}}{2} \\ \bar{x}_i = \dfrac{x_i - x_{\text{mid}}}{0.5(x_{\max} - x_{\min})}, i = 1, 2, \cdots, N \end{cases} \tag{22}$$

where x_i is the input sample data. $x_{\max}$ is the maximum value of the sample data. $x_{\min}$ is the minimum value of the sample data. x_{mid} is the middle value of the sample data. $\bar{x}_i$ is the normalized sample data, and N is the sample data volume. After normalization according to Eq. (22), the median value of the input sample data is 0, and the minimum and maximum values of the sample data are -1 and 1 respectively.

3.2.4. Training process and results

The parameter settings of the neural network training are as shown in Table 2.

Figs. 15 and 16 show the training process and linear regression results of the SPM model respectively. The input parameters of the training set, test set and verification set are substituted into the model, and the predicted output results of the model are compared with the actual data. the residuals of the turning parameters k_x, k_y, k_z are obtained as shown in Figs. 17–19. From the training process and the residual diagram, it can be seen the trained neural network can adapt to state changes, the model error is small, and the mapping relationship between state and parameters is well fitted. At the same time, due to the deflected parameters of the missile, the generalization of the model is also guaranteed.

Table 2
Network setting.

Network setting	Function/Value
The loss function	Mean Square Error
The training algorithm	Levenberg-Marquardt
The activation function	The Tan-Sigmoid transfer function
The output layer	The linear activation function
The maximum number of training sessions	1000
The accuracy required	1e-6

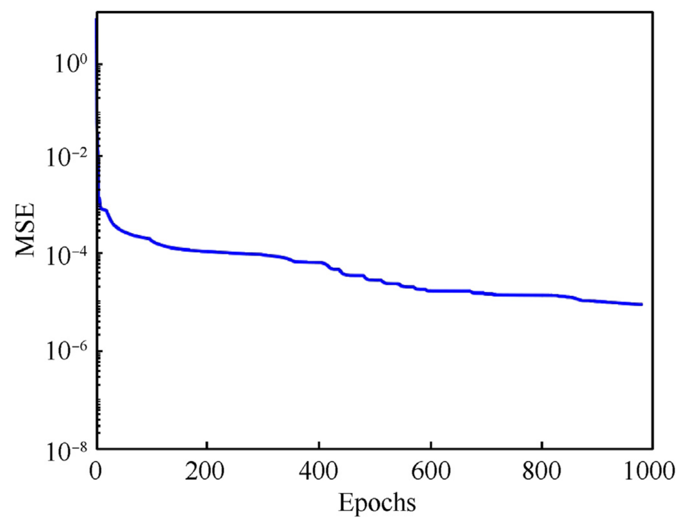

Fig. 15. The training process.

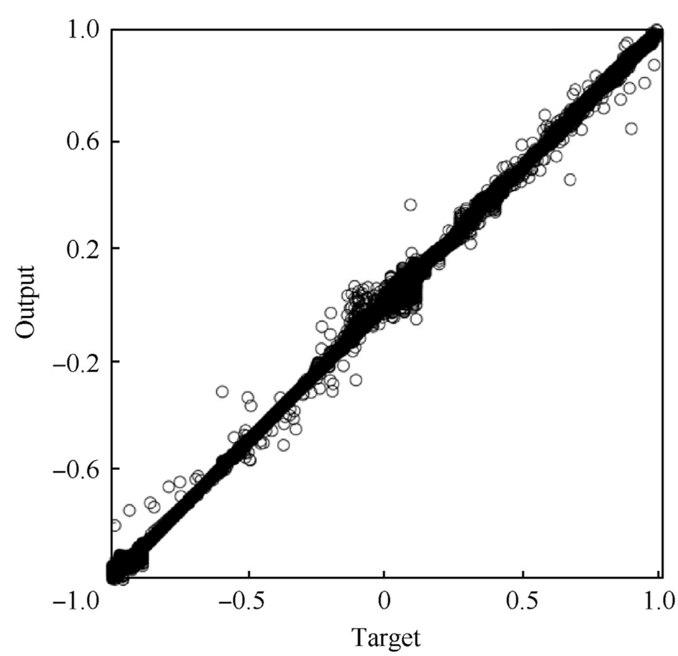

Fig. 16. The linear regression results.

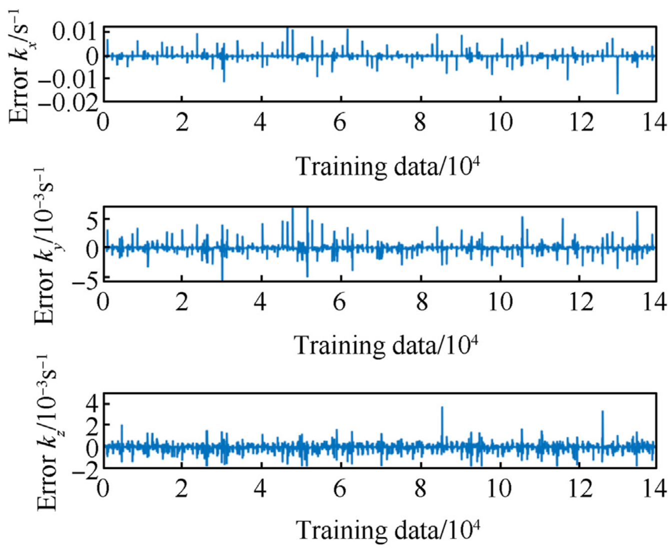

Fig. 17. The residuals of ***K*** in the training set.

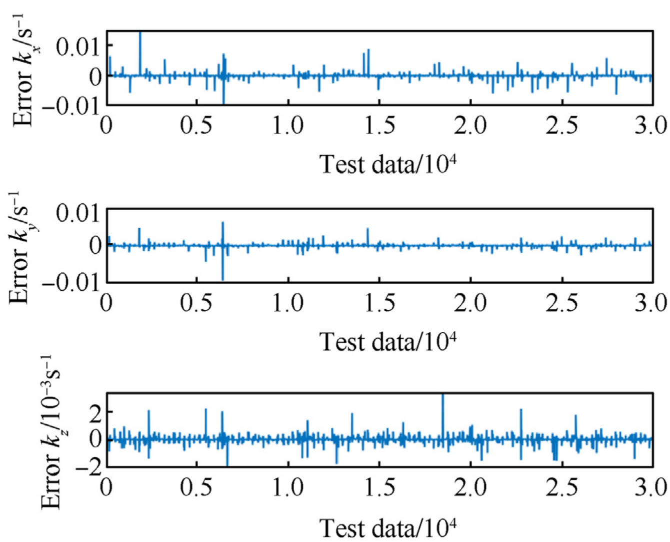

Fig. 18. The residuals of ***K*** in the test set.

3.3. Online trajectory prediction

For the trajectory of the ballistic missile predicted online, when the tracker estimates the continuous state to the start of the forecast, the established the SPM model is started to predict and reconstruct the trajectory. Specifically, according to the state $\boldsymbol{X}_t$ of the predicted start moment, $\boldsymbol{K}_t$ of the predicted start moment can be obtained by the SPM model. Then the state $\boldsymbol{X}_{t+1}$ of the next moment is obtained through the T3 model, it is continue fed into the SPM model to obtain $\boldsymbol{K}_{t+1}$ of the next moment. By analogy, the predicted trajectory of a ballistic missile can be obtained at any $T > t$ time. The online trajectory prediction and update scheme is shown in Fig. 20.

4. Simulation analysis

4.1. Simulation settings

The ballistic missile in subsubsection 3.2.3 is taken as the

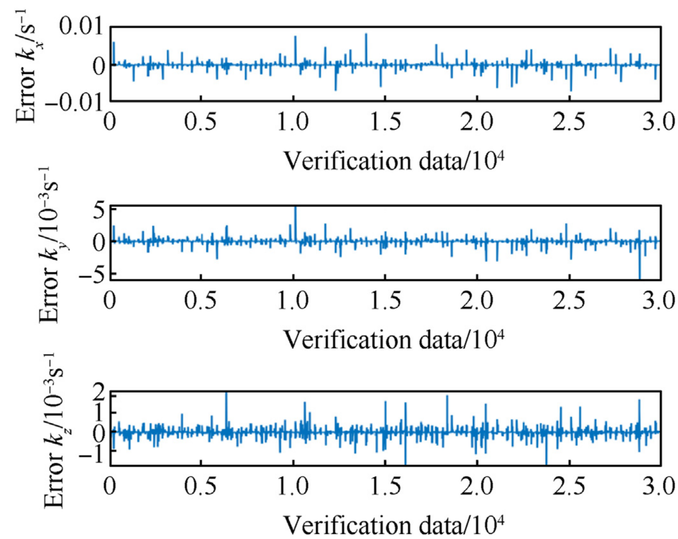

Fig. 19. The residuals of ***K*** in the verification set.

research object. In the range of launch point and target point, two trajectories are generated based on standard missile parameters and deflected missile parameters respectively, which are used to verify the DKTP algorithm. At the same time, in order to verify the applicability of the algorithm, by planning the missile launch data, the trajectory generated based on the deflected parameters has stronger maneuverability. The trajectory parameters are shown in Table 3.

The trajectory curves of the boost phase are shown in Figs. 21–26. Case 1 is the target trajectory based on the standard parameter planning. Case 2 is the target trajectory based on the deflected parameter planning. It can be seen that compared with Case 1, the target trajectory of Case 2 has stronger maneuverability, and the acceleration mutation is more obvious. Two trajectories with completely different shapes can effectively verify the accuracy, robustness and stability of the trajectory prediction algorithm.

Table 4 shows the parameters of the infrared detector.

The parameters of the trajectory prediction are shown in Table 5.

4.2. Simulation of trajectory tracking

Figs. 27–30 is the target trajectory tracking result of Case 1. Figs. 31–34 is the target trajectory tracking result of Case 2. It can be seen from Figs. 27–30 that the pure geometric positioning error is about 400 m, the position tracking error can be stabilized below 100 m, and the velocity tracking error is gradually converging to about 20 m s^{-1}. It shows that the tracking scheme based on air-based dual infrared detectors has a significant effect, which can effectively reduce the pure geometric positioning error.

It can be seen from Figs. 31–34 that the tracking accuracy is still high in the case of trajectory parameter deviation. It fully shows that the tracking scheme based on space-based dual infrared detector has high accuracy and strong stability.

4.3. Case 1

The following is the comparative simulation of trajectory prediction in the boost phase under Case 1. The algorithms involved in the comparison include.

1) The DKTP algorithm: Trajectory prediction algorithm driven by data and knowledge proposed in this paper. BP neural network

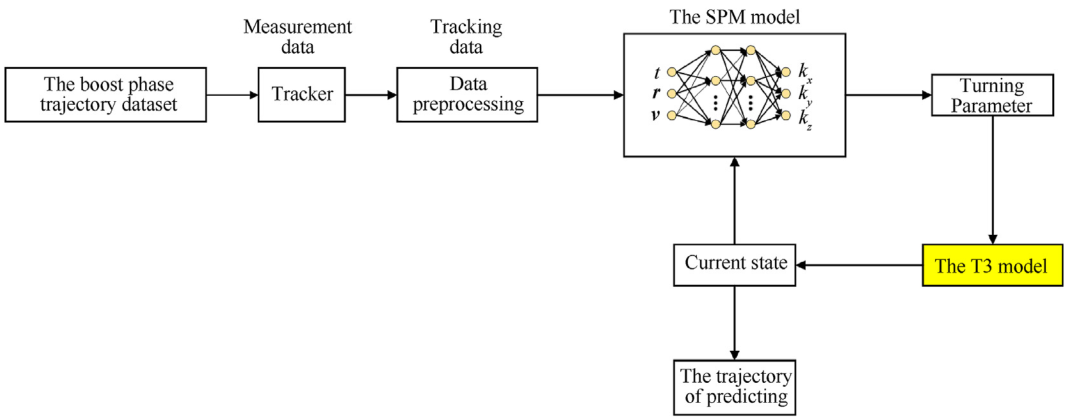

Fig. 20. Flowchart of online trajectory prediction and update scheme.

Table 3
Trajectory parameters.

Parameters	Case 1	Case 2
Longitude of the launch point/(°)	48.80	45.94
Latitude of the launch point/(°)	15.24	19.06
Altitude of the launch point/m	573.2	259.46
Longitude of the target point/(°)	60.85	62.93
Latitude of the target point/(°)	49.5	51.60
Altitude of the target point/m	0.58	0.33
Range/km	3954.6	3905.5
Launch azimuth/(°)	13.28	18.95
Limited angle of attack/(°)	9.78	5.78
Aiming angle of attack/(°)	3.54	36.10
Moment of the end point of the boost phase/s	201	205.9

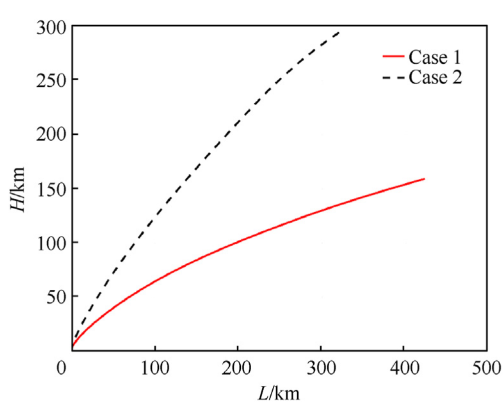

Fig. 21. The range height curve.

is used to train the three-dimensional turning coefficient $\boldsymbol{K}$ of the target, and combined with the three-dimensional turning model for trajectory prediction.

2) The GT-BP algorithm: BP neural network is used to train the target gravity turning coefficient k, and combined with the gravity turning model for trajectory prediction. It belongs to the trajectory prediction algorithm driven by data and knowledge.
3) The T3-PCFTPA algorithm: The three-dimensional turning is combined with the polynomial curve fitting trajectory prediction algorithm. The three-dimensional turning coefficient $\boldsymbol{K}$ is fitted for trajectory prediction. It belongs to knowledge-driven trajectory prediction algorithm.
4) The GT-PCFTPA algorithm: The gravity turning model is combined with polynomial curve fitting trajectory prediction

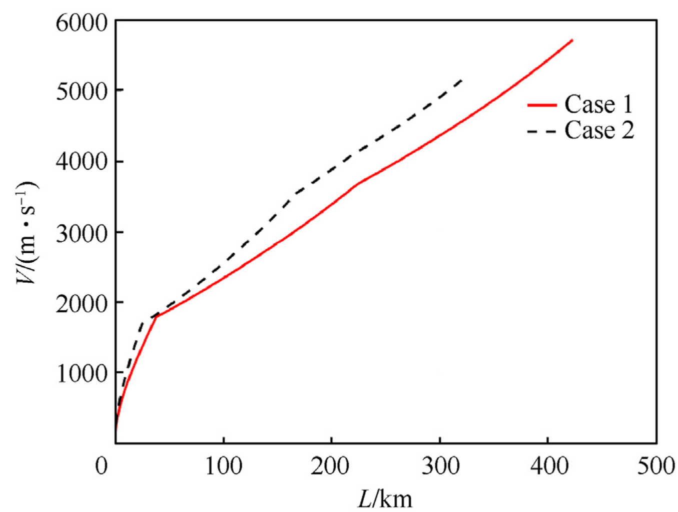

Fig. 22. The range velocity curve.

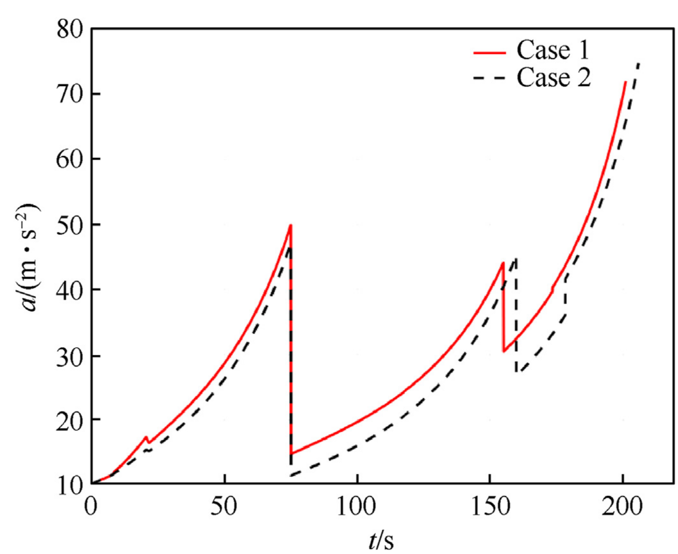

Fig. 23. The acceleration curve.

algorithm. The gravity turning coefficient k is fitted for trajectory prediction. It belongs to knowledge-driven trajectory prediction algorithm.

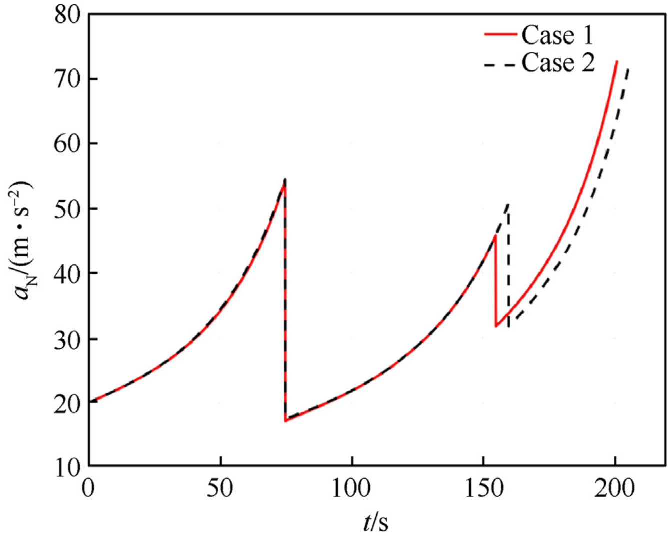

Fig. 24. The nongravitational net acceleration curve.

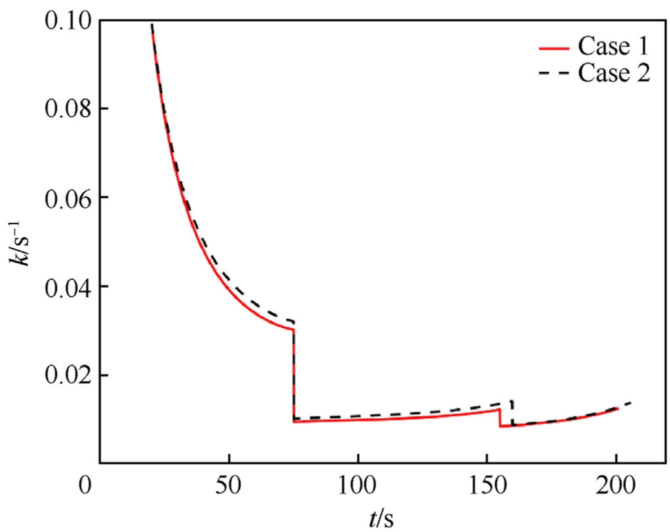

Fig. 25. The gravitational turning parameter curve.

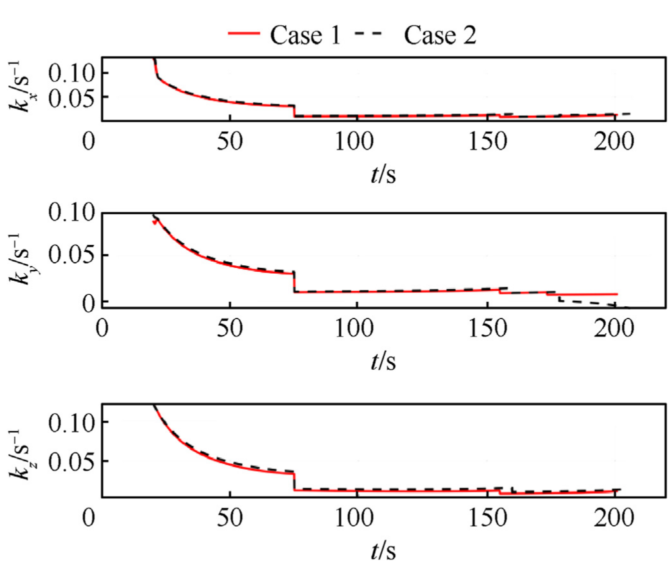

Fig. 26. The three-dimensional turning parameter curve.

Table 4
Parameters of infrared detector.

Parameters	Case 1	Case 2
Longitude of the first detector/(°)	48.79	45.94
Latitude of the first detector/(°)	14.25	18.06
Altitude of the first detector/km	10	10
Longitude of the second detector/(°)	48.79	45.94
Latitude of the second detector/(°)	16.25	20.06
Altitude of the second detector/km	10	10
Baseline length/km	220	220
Maximum detection distance/km	500	500
Detection accuracy/mrad	1	1

Table 5
Parameters of the trajectory prediction.

Parameter	Value
The start moment of tracking/s	60
The start moment of predicting/s	80
The end moment of predicting/s	201

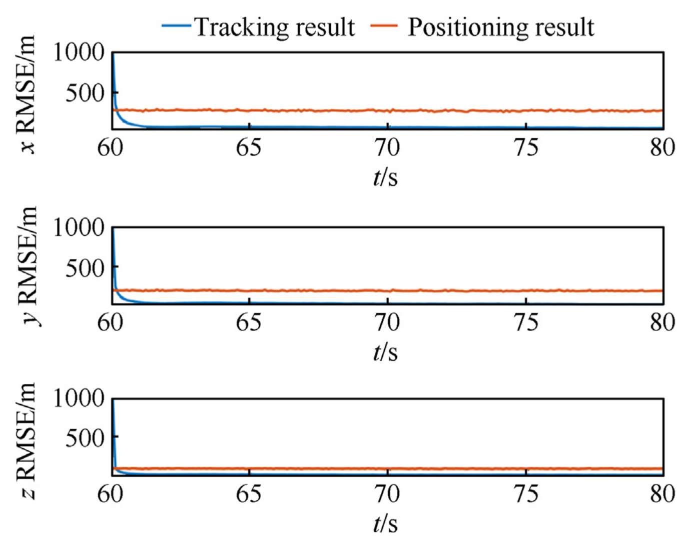

Fig. 27. Three-dimensional position error of trajectory tracking under Case 1.

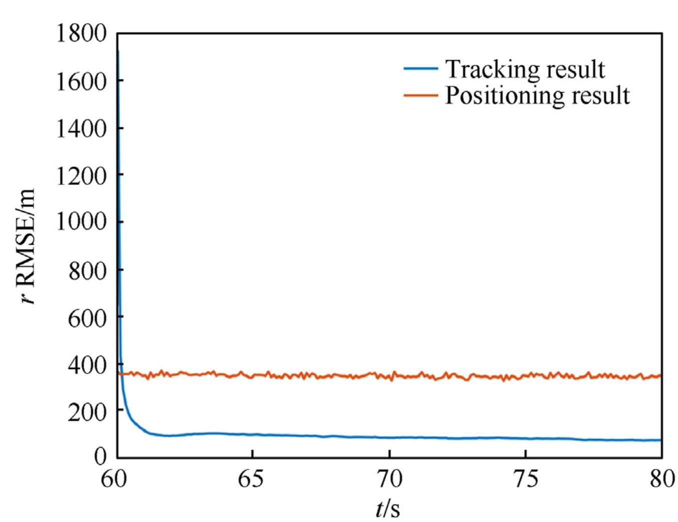

Fig. 28. Position error of trajectory tracking under Case 1.

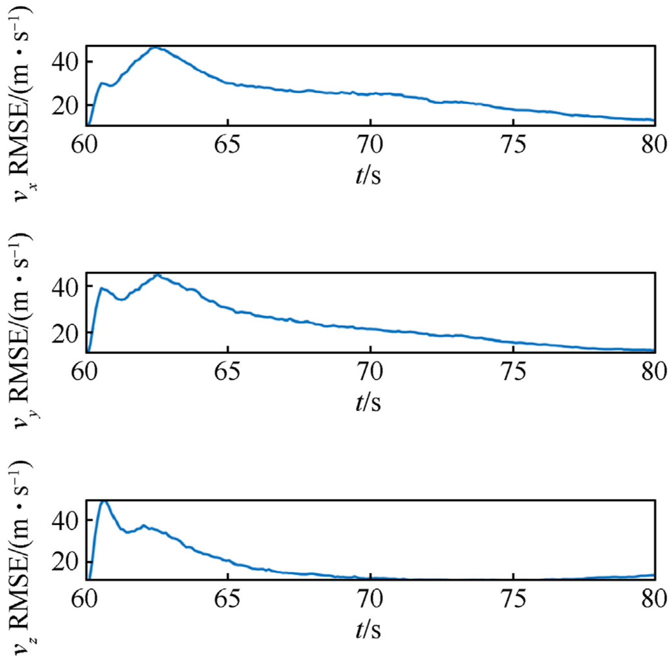

Fig. 29. Three-dimensional velocity error of trajectory tracking under Case 1.

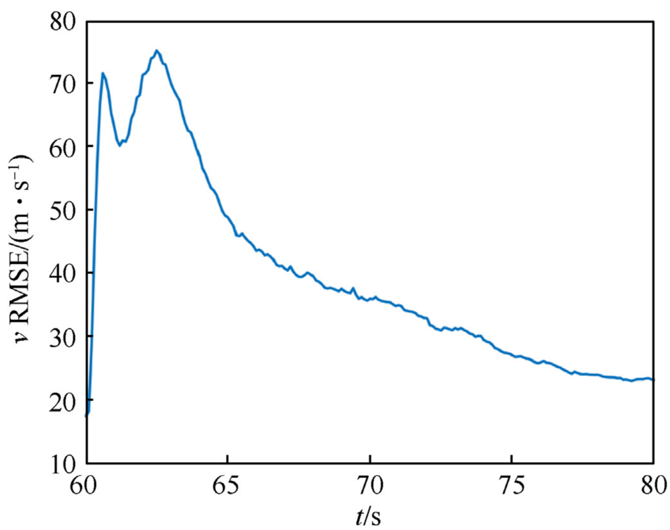

Fig. 30. Velocity error of trajectory tracking under Case 1.

5) The RNN trajectory prediction algorithm: Recurrent neural network is used to predict the target state. The RNN trajectory prediction algorithm belongs to data-driven trajectory prediction algorithm.
6) The LSTM trajectory prediction algorithm: Long short-term memory neural network is used to predict the target state. It belongs to data-driven trajectory prediction algorithm.

The trajectory prediction results of 1000 Monte Carlo shots are shown in Figs. 35–38.

It can be seen that with the increase of prediction time, the six algorithms have different degrees of divergence. Among them, the T3-PCFTPA algorithm and GT-PCFTPA algorithm based on pure knowledge-driven have the highest degree of divergence. When

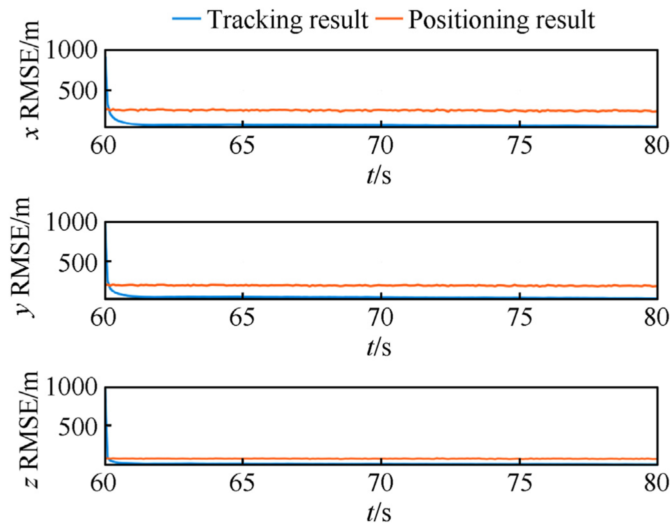

Fig. 31. Three-dimensional position error of trajectory tracking under Case 2.

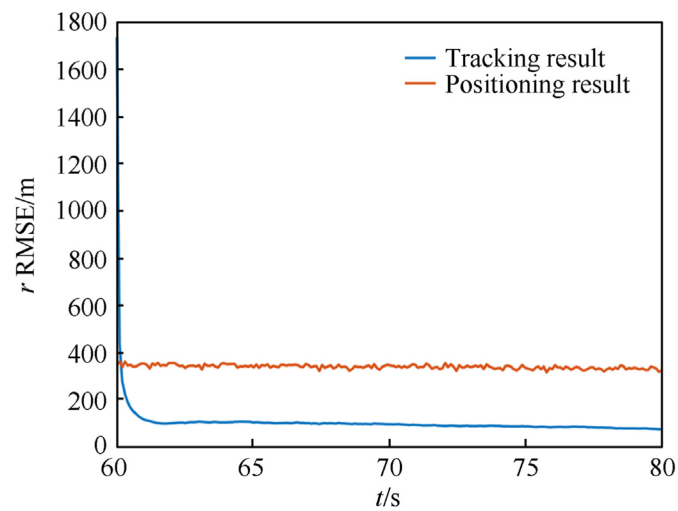

Fig. 32. Position error of trajectory tracking under Case 2.

the second stage booster is switched to the third stage booster within 155 s, the RMSE curve of the speed prediction fluctuates significantly. The accuracy of the RNN trajectory prediction algorithm and the LSTM trajectory prediction algorithm based on pure data-driven is slightly improved, and the speed RMSE curves fluctuate less during inter-stage switching. This is because the use of a large amount of data for training effectively reduces the prediction error caused by the sudden change of target acceleration. The prediction accuracy of the GT-BP algorithm is comparable to that of the LSTM trajectory prediction algorithm. Because the GT model cannot accurately describe the target maneuver, resulting in limited improvement in prediction accuracy. Due to the combination of data-driven and knowledge-driven advantages, the DKTP algorithm has the highest trajectory prediction accuracy and the best algorithm stability. From the velocity RMSE curves, it can be seen that compared with other algorithms, the DKTP algorithm can accurately describe the maneuvering characteristics of the ballistic missile boost phase, which is more sensitive to the three-dimensional acceleration change of the boost phase.

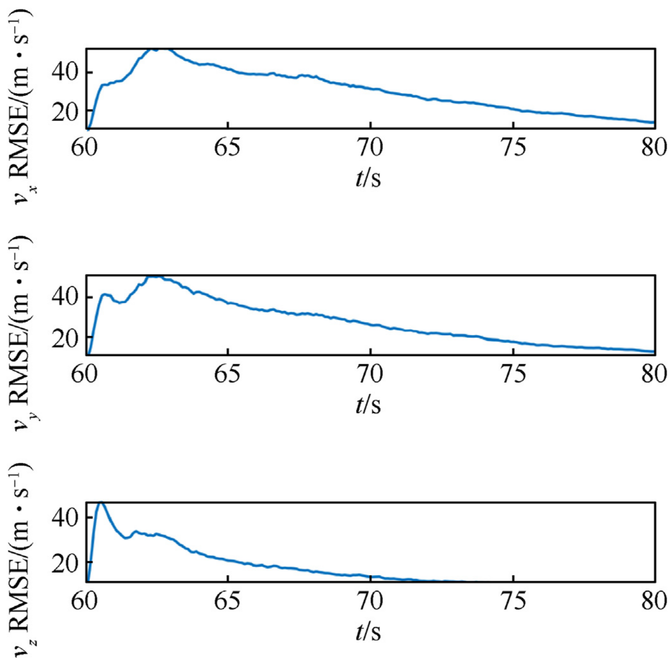

Fig. 33. Three-dimensional velocity error of trajectory tracking under Case 2.

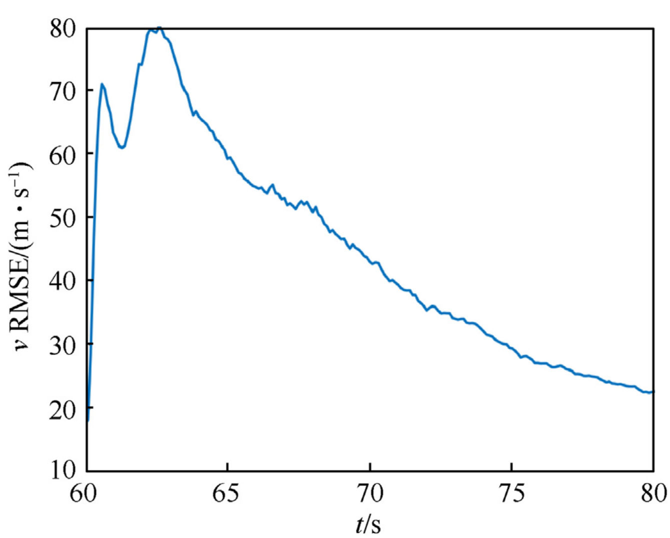

Fig. 34. Velocity error of trajectory tracking under Case 2.

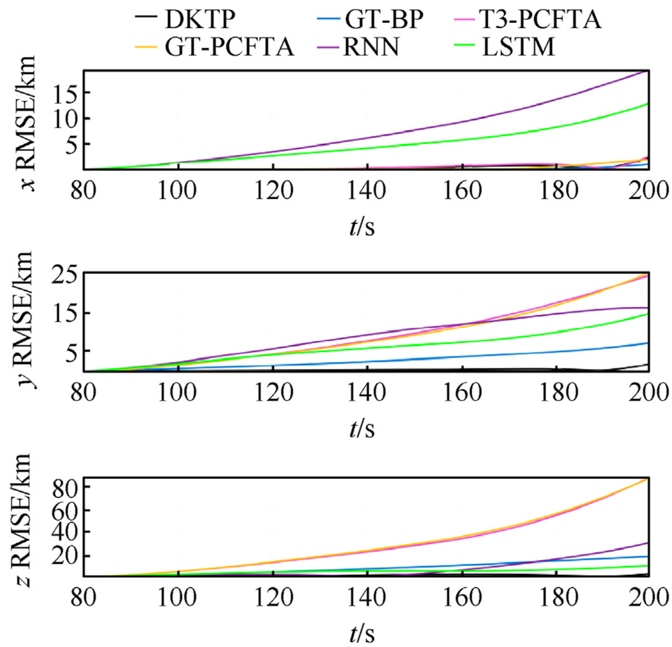

Fig. 35. RMSE of the three-dimensional location prediction.

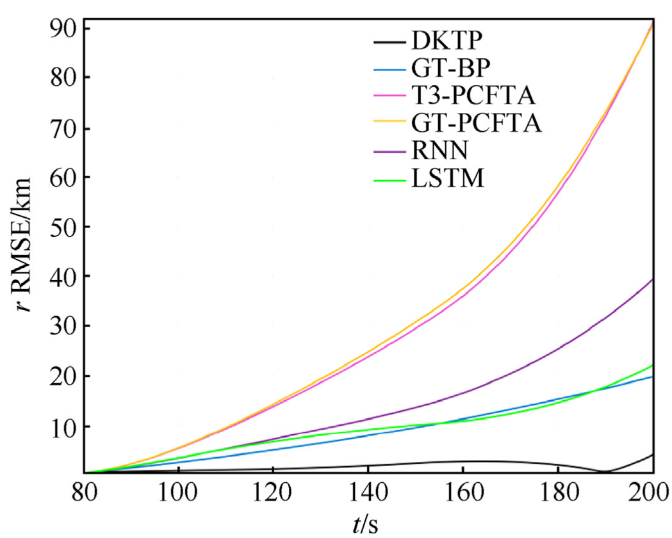

Fig. 36. RMSE of the location prediction.

4.4. Case 2

The comparative simulation results of trajectory prediction in the boost phase under Case 2 are shown in Figs. 39–42. The algorithm involved in the comparison is the same as Case 1.

As shown in Figs. 39 and 40, when the missile parameters are deviated and the acceleration of the aiming segment increases suddenly, the position prediction errors of these six algorithms increase significantly. However, the DKTP algorithm proposed in this paper can still control the position prediction error at about 10 km when the boosting phase ends. As shown in Figs. 41 and 42, when the 155 s inter-stage switching and 173 s flight mode switching, the speed prediction RMSE curves of other algorithms except the DKTP algorithm fluctuate more violently. For the DKTP algorithm, although the flight mode switching will also cause the RMSE of the speed prediction to fluctuate, the fluctuation is not large and can be called back quickly. This is because the three-dimensional turning model can accurately describe the acceleration mutation of the boost phase. When combined with the BP neural network, the mapping relationship between the three-dimensional turning coefficient ***K*** and the motion state can be accurately established. Therefore, the DKTP algorithm has the best prediction effect on the trajectory of the boost phase. It fully shows that when the DKTP algorithm predicts the trajectory of non-cooperative targets, even if the accurate target parameters cannot be obtained, the trajectory prediction accuracy can still be guaranteed.

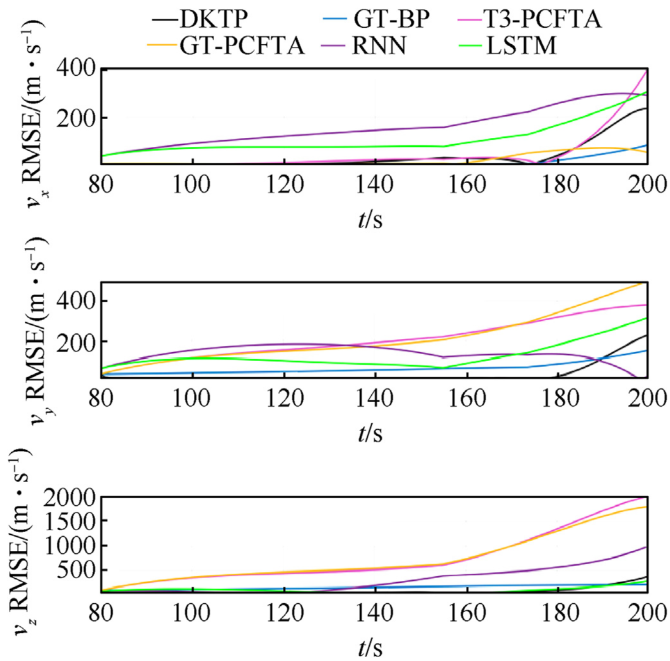

Fig. 37. RMSE of the three-dimensional velocity prediction.

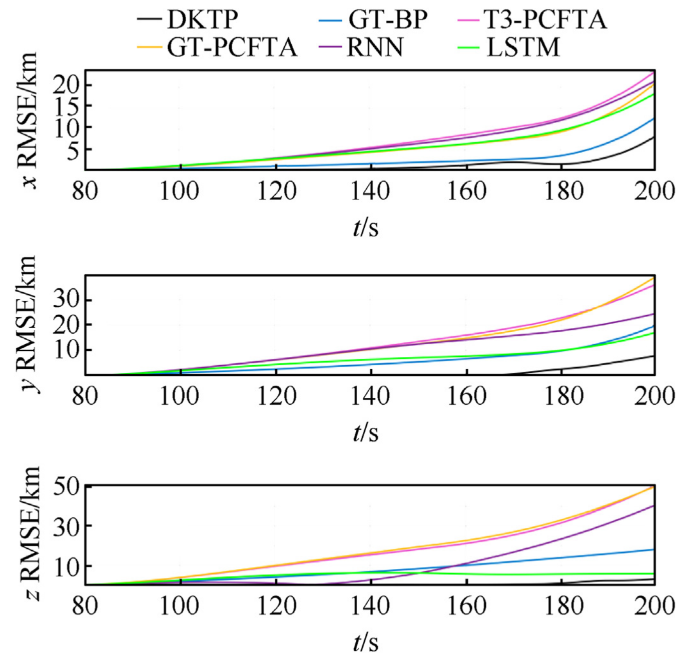

Fig. 39. RMSE of the three-dimensional location prediction.

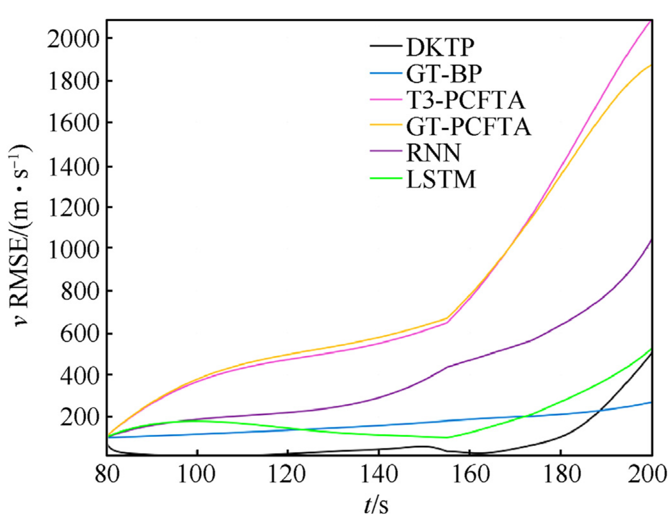

Fig. 38. RMSE of the velocity prediction.

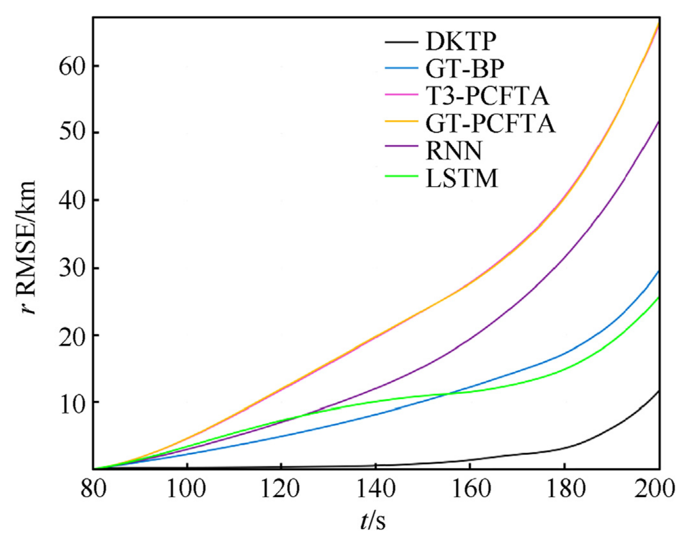

Fig. 40. RMSE of the location prediction.

5. Conclusions

Aiming at the problem of high-precision trajectory prediction in the boost phase of multi-stage ballistic missiles, this paper proposes a trajectory prediction method driven by data and knowledge. In order to cope with acceleration abrupt change in the boost phase, this paper combines the dynamics model of the boost phase with the target gravity turning model to derive the three-dimensional turning model of the target. Then, by combining the dynamic model of the boost phase and the three-dimensional model, the three-dimensional turning parameter in the boost phase is extracted. The three-dimensional turning parameter changes during the flight in the boost phase are analyzed, and the analysis results show it can accurately reflect the thrust change in the boost phase engine and the change of flight program. On this basis, the relationship between the three-dimensional turning parameter and the flight state in the boost phase is derived. Using the BP neural network to train the trajectory database in the boost phase, and the state-parameter mapping model is established. The state-parameter mapping model takes the current state of the target as the input and the three-dimensional turning parameter of the target as the output. Thanks to the strong nonlinear fitting ability of the BP neural network and the accurate description of the acceleration mutation of the boost phase by the three-dimensional turning model, the trajectory prediction algorithm driven by data and knowledge uses the turning coefficient mapped by the current moment state to predict the state of the next moment, and continuously extrapolates to realize the online prediction of the trajectory. Finally, under the condition of different aiming angles of attack, that is, different degrees of maneuver in the boost phase, the trajectory prediction algorithm driven by data and knowledge proposed in this paper is compared and simulated. The simulation

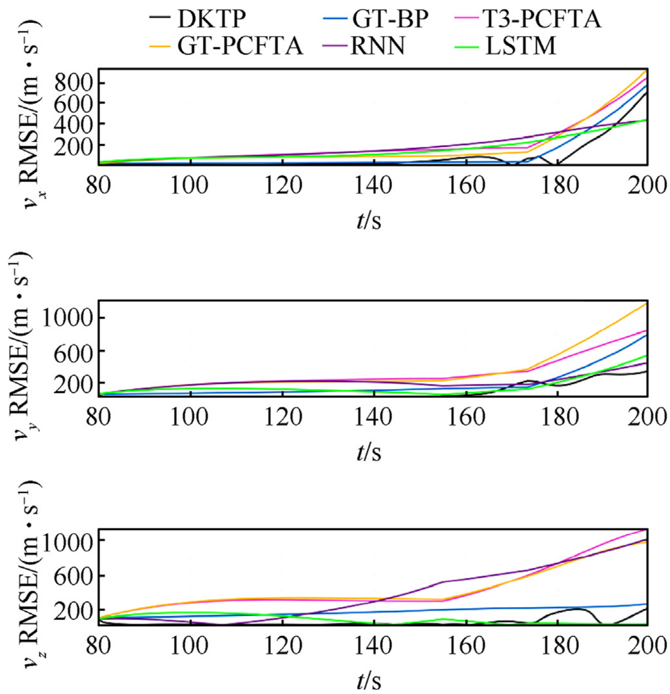

Fig. 41. RMSE of the three-dimensional velocity prediction.

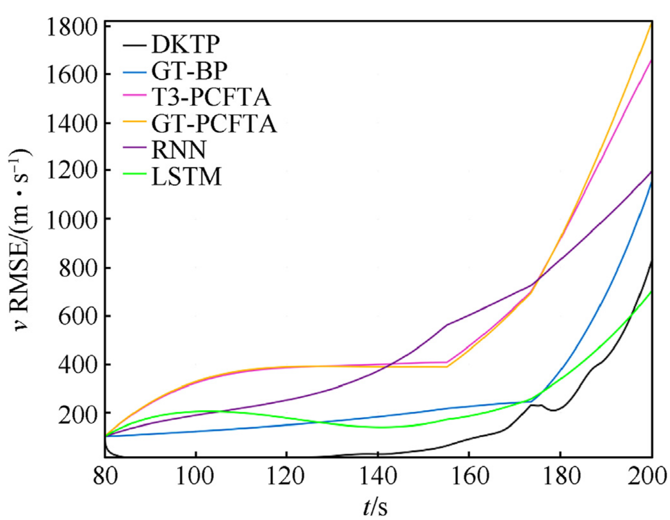

Fig. 42. RMSE of the velocity prediction.

results show that the DKTP algorithm combines data-driven and knowledge-driven, makes full use of their respective advantages, and effectively enhances the performance of the algorithm. The trajectory prediction algorithm driven by data and knowledge uses the state-parameter mapping model, which makes up for the shortcomings of the knowledge-driven method under the condition of complex target motion model and flight environment uncertainty. At the same time, the physical significance of the data-driven method is clarified by using the three-dimensional turning model and the three-dimensional turning parameter. It can effectively alleviate the adverse effects of acceleration abrupt change of the trajectory prediction in the boost phase, and can significantly improve the trajectory prediction accuracy of ballistic missiles in the boost phase, which has certain engineering application value.

CRediT authorship contribution statement

Hongyan Zang: Writing – review & editing, Writing – original draft, Data curation. **Changsheng Gao:** Project administration, Funding acquisition. **Yudong Hu:** Project administration, Funding acquisition. **Wuxing Jing:** Project administration.

Declaration of competing interest

The authors declare that they have no known competing financial interests or personal relationships that could have appeared to influence the work reported in this paper.

Acknowledgements

The authors would like to acknowledge the National Natural Science Foundation of China (Grants No. 12072090 and No. 12302056) to provide fund for conducting experiments.

References

[1] Persico R, Ilioudis CV, Clemente C, Soraghan JJ. Novel classification algorithm for ballistic target based on HRRP frame. IEEE Trans Aero Electron Syst 2019;55(6):3168–89.
[2] Lee D, Cho K. Shin. A simple prediction method of ballistic missile trajectory to designate search direction and its verification using a testbench. In: 2015 10th asian control conference (ASCC); May. 31-Jun. 3, 2015. Kota Kinabalu, Malaysia.
[3] Chen W, Hu Y, Gao C, An R. Trajectory tracking guidance of interceptor via prescribed performance integral sliding mode with neural network disturbance observer. Def. Technol. 2024;32:412–29.
[4] Yu M, Chen WH, Chambers J. State dependent multiple model-based particle filtering for ballistic missile tracking in a low-observable environment. Aero Sci Technol 2017;67:144–54.
[5] Qiu X, Lai P, Gao C, Jing W. Recorded recurrent deep reinforcement learning guidance laws for intercepting endoatmospheric maneuvering missiles. Def. Technol. 2024;31:457–70.
[6] Jung Y, Lee H, Lee Y, Kim Y, Ahn J. Composite zero-effort-miss guidance with predictor–corrector steps for ballistic interception. J Guid Control Dynam 2024;47(2):311–25.
[7] Wang S, Guo Y, Wang S, Liu Z, Zhang S. Cooperative interception with fast multiple model adaptive estimation. Def. Technol. 2021;17:1905–17.
[8] Xian Y, Ren L, Xu Y, Li S, Wu W, Zhang D. Impact point prediction guidance of ballistic missile in high maneuver penetration condition. Def. Technol. 2023;26:213–30.
[9] Zhang X, Lei H, Li J, Zhang D. Ballistic missile trajectory prediction and the solution algorithms for impact point prediction. In: 2014 IEEE Chinese guidance, navigation and control conference guidance; Aug. 08-10, 2014. Yantai, China.
[10] Li XR, Jilkov VP. Survey of maneuvering target tracking. Part II: motion models of ballistic and space targets. IEEE Trans Aero Electron Syst 2010;46(1):96–119.
[11] Jing W, Yang B, Gao C. Review on guidance technology of air-based missiles for boost phase interception. J Harbin Inst Technol 2021;53(6):1–12.
[12] Ann S, Lee S, Kim Y, Ahn J. Midcourse guidance for exoatmospheric interception using response surface based trajectory shaping. IEEE Trans Aero Electron Syst 2020;56(5):3655–73.
[13] Lin Y, Lin C, Suebsaiprom P, Hsieh S. Estimating evasive acceleration for ballistic targets using an extended state observer. IEEE Trans Aero Electron Syst 2016;52(1):337–49.
[14] Zarchan P. Kill vehicle guidance and control sizing for boost-phase intercept. J Guid Control Dynam 2011;34(2):513–21.
[15] Jang S, Hutchins R, Pace P. Boost phase ICBM engagement using space-based interceptors: a comparison of guidance laws. In: 2008 IEEE international conference on system of systems engineering system of systems engineering, CA, USA, jun; 2008. p. 2–4.
[16] Ji R, Zhang C, Liang Y, Wang Y. Trajectory prediction of boost-phase ballistic missile based on LSTM. Syst Eng Electron 2022;4(6):1968–76.
[17] John A, Lukacs IV, Yakimenko OA. Trajectory-shaping guidance for interception of ballistic missiles during the boost phase. J Guid Control Dynam 2008;31(5):1524–31.
[18] Geng L, Wu N, Meng F, Han J. A analytical method of trajectory prediction considering J2 perturbations and including short-period terms. In: 2018 4th international conference on control, automation and robotics (ICCAR); Apr. 20-23, 2018. Auckland, New Zealand.
[19] Harlin WJ, Cicci DA. Ballistic missile trajectory prediction using a state transition matrix. Appl Math Comput 2007;188(2):1832–47.
[20] Yu W, Yang J, Chen W, Liao B, Zhu H. Analytical trajectory prediction for near-

first-cosmic-velocity atmospheric gliding using a perturbation method Acta. Astronautics 2021;187:79–88.
[21] Hu Y, Gao C, Li J, Jing W. Maneuver mode analysis and parametric modeling for hypersonic glide vehicles. Aero Sci Technol 2021;119:107166.
[22] Ahn J, Seo J. Instantaneous impact point prediction using the response-surface method. J Guid Control Dynam 2013;36(4):958–66.
[23] Li F, Xiong J, Lan X, Bi H, Tan X. Hypersonic vehicle trajectory prediction algorithm based on Hough transform. Chin J Electron 2021;30(5):918–30.
[24] Hu Y, Gao C, Li J, Jing W, Li Z. Novel trajectory prediction algorithms for hypersonic gliding vehicles based on maneuver mode on-line identification and intent inference. Meas Sci Technol 2021;3(11):115012.
[25] Zhang P, Sun Y, Lin Z, Li X. Method of flight trajectory prediction of a missile based on the polynomial prediction. Tactical Missile Technol 2013;2:35–7.
[26] Fan Y, Tan Y, Wu L, Ye H, Lyu Z. Global and local interattribute relationships-based graph convolutional network for flight trajectory prediction. IEEE Trans Aero Electron Syst 2024;60(3):2642–57.
[27] Xie Y, Zhuang X, Xi Z, Chen H. Dual-channel and bidirectional neural network for hypersonic glide vehicle trajectory prediction. IEEE Access 2021;9: 92913–24.
[28] Peng H, Bai X. Gaussian processes for improving orbit prediction accuracy. Acta Astronaut 2019;161:44–56.
[29] Moon IC, Song K, Kim SH, Choi HL. State prediction of high-speed ballistic vehicles with Gaussian process. Int. J. Control. Autom. 2018;16(3):1282–92.
[30] Xi Z, Kou Y, Li Z, Lv Y, Xu A, Li Y, et al. Air combat target maneuver trajectory prediction based on robust regularized Volterra series and adaptive ensemble online transfer learning. Def. Technol. 2023;20:187–206.
[31] Qian K, Zhou Y, Yang L, Xie R, He X. Aircraft target track prediction model based on BP neural network. Command. Inf. Syst. Technol. 2017;8(2):54–8.
[32] Song B, Xu G. Missile trajectory prediction method based on LSTM and IDCNN. Syst Eng Electron 2023;45(2):504–12.
[33] Ji R, Liang Y, Xu L, Wei Z. Trajectory prediction of ballistic missiles using Gaussian process error model. Chin J Aeronaut 2022;35(1):458–69.
[34] Zhang B, Zhu J, Su H. Toward the third generation of artificial intelligence. Scientia. Sinica. Inf. 2020;50(9):1281–302.
[35] Feng T, Liu Y, Yu Y, Chen L, Chen R. A data and physical model dual-driven based trajectory estimator for long-term navigation. Def. Technol. 2024;40: 78–90.
[36] Huang X, Liu J, Zhang Y, Zhang H, Jia C, Liu X. Review on knowledge-based and data-driven cooperating control methods of high-speed vehicle. J. Astronaut. 2023;44(8):1113–26.
[37] Wu N, Chen L, Lei Y, Meng F. Adaptive estimation algorithm of boost-phase trajectory using binary asynchronous observation. Proc Inst Mech Eng Part G-J Aerosp Eng 2016;230(14):2661–72.
[38] Hou P, Pei Y, Ge Y. Adaptive fuze-warhead coordination method based on BP artificial neural network. Def. Technol. 2023;(19):117–33.